



# Coal Damage and Permeability Characteristics Under Accelerated Unloading Confining Pressure

Kai Wang · Xiang Zhang · Feng Du · Chengpeng Xin · Liang Wang

Received: 1 January 2019 / Accepted: 31 August 2019 / Published online: 4 September 2019  
© Springer Nature Switzerland AG 2019

**Abstract** Based on the actual mining conditions and the stress state of coal on-site, the damage–permeability–acoustic emission (AE) experiments of gas-bearing raw coals were carried out under the conditions of conventional triaxial unloading (UCP) and accelerated unloading confining pressure (AUCP) with different gas pressures and confining pressures. The effects of unloading speeds increasing during the process of unloading confining pressure on the damage and permeability of coals were analyzed. Meanwhile, the intrinsic mechanism of the coal damage and permeability evolution in front of the working face is revealed. The results show that under the two unloading paths, the failure mode is both the tension–shear failure. The AE signals correspond well with the

stress–strain and permeability evolutions of the coal samples. At the initial stage, the AE signal is relatively less, and it rises sharply when the coal approaches instability and failure, presenting the characteristics of rapid damage as a whole. Compared with UCP, AUCP has a greater impact on the damage and permeability characteristics of raw coal. The acute damage of coal is more severe and the time required for reaching instability and failure is significantly shortened under AUCP. The permeability increment under AUCP is obviously higher than that under UCP. When the sample is damaged, the unloading ratio of confining pressure is smaller under AUCP, and the sample shows more broken and more impact destructive effect. With the increase of initial confining pressure

---

K. Wang · X. Zhang · F. Du (✉) · C. Xin · L. Wang  
Beijing Key Laboratory for Precise Mining of Intergrown Energy and Resources, China University of Mining and Technology (Beijing), Beijing 100083, China  
e-mail: fengducumtb@126.com

X. Zhang  
e-mail: xzcumtb@126.com

K. Wang · X. Zhang · F. Du · C. Xin · L. Wang  
College of Emergency Management and Safety Engineering, China University of Mining and Technology (Beijing), Beijing 100083, China

K. Wang  
Hebei State Key Laboratory of Mine Disaster Prevention, North China Institute of Science and Technology, Beijing 101601, China

F. Du  
Department of Civil Engineering and Engineering Mechanics, Columbia University, New York, NY 10027, USA

C. Xin  
School of Mining Engineering, Guizhou University of Engineering Science, Bijie 551700, China

or the decrease of gas pressure, the time required for instability and failure increases, and the influence of accelerated unloading path on coal is strengthened. Therefore, the accelerated advancement of working face is more likely to induce coal gas dynamic disasters.

**Keywords** Gas-bearing coal · Accelerated unloading · Damage · Permeability · Acoustic emission

## 1 Introduction

Coal is an important energy source in the world, which has an increasing demand. In recent years, the mining depth in China increases gradually and the mining depths even exceed 1000 m in some mines (Lama and Bodziony 1998; Wold et al. 2008; Xie et al. 2017; Wang and Du 2019a). As a result, the difficulty of gas disasters control is further increased, and the risk of coal gas dynamic disasters is enhanced (Du and Wang 2019; Fan et al. 2017). During the advancing process of the working face, the coal body ahead is mainly subjected to the mechanical action of unloading confining pressure (Chen et al. 2013, 2014; Qian et al. 2018; Yin et al. 2015). Meanwhile, the mechanical and permeability characteristics of the coal body will change significantly with the variation of stress and time (Wierzbicki et al. 2014; Wang et al. 2017a). Therefore, it is of great significance to study the mechanism of deformation, failure and seepage evolution of coal under accelerated unloading confining pressure, which plays a key role in the prevention and control of coal gas dynamic disasters.

There are a lot of researches focusing on the mechanical behavior and permeability characteristics of coals under unloading. Chen et al. (2013, 2014) studied the damage and permeability characteristics of gas-bearing coals under two different unloading paths which makes a lot of sense in protective seam mining. Yin et al. (2015), Zhang et al. (2018a) and Xue et al. (2017) studied the impacts of the rates of unloading confining pressure on the damage and seepage characteristics of gas-bearing coals. They stated that the higher unloading rates, the lower peak strength and the greater permeability. Liu et al. (2017) conducted the numerical assessment of the permeability evolutions

under the condition of geostress-relief corresponding to the remote unloading mining. They stated that unloading mining will lead to the increasement of coal permeability and improve gas extraction amount. Zhang et al. (2018b) investigated the seepage law of gas-bearing raw coal under different stress conditions and presented that the flow rate of gas in the coal increases with the nonlinear unloading. Jiang et al. (2017) carried out an experimental study on mechanical and permeability characteristics of gas-bearing coal with a certain ratio of axial loading speed to confining pressure unloading speed. It was found that the strength of coal increased logarithmically with the increase of initial hydrostatic pressure and decreased exponentially with the increase of loading/unloading speed. Besides, other scholars (Pan and Connell 2011; Wang and Du 2019b; Xie et al. 2012; Zhang et al. 2017) also systematic studied the mechanical or permeability properties of coals under unloading confining pressure through triaxial compression tests. It can be seen from the above literatures that little attention has been paid to the influence of the changing unloading speed's changing during the process of unloading confining pressure on the damage and permeability of gas-bearing coal. In the actual coal mining face advancing, the mining speed is not fixed. Sometimes, the face will be accelerated to improve the production efficiency. However, the typical coal and rock dynamic disasters such as coal–gas outburst and rockburst are likely to occur when the speed is faster awhile or slower awhile. Especially in recent years, many deep mines often have coal and gas dynamic phenomena under the action of high ground stress, high gas pressure, mining disturbance and other factors. At present, the relationship between accelerated advance of working face and induced dynamic disaster is still unclear, so it is necessary to study the damage and permeability law of gas-bearing coal under accelerated unloading confining pressure.

In this work, the change of stress field in front of coal body under accelerated advancing of working face was simplified. The damage–permeability experiments of gas-bearing raw coal were conducted by conventional triaxial unloading (UCP) and accelerated unloading confining pressure (AUCP) under different gas pressures and confining pressures. The effects of increasing unloading speeds increasing during the process of unloading confining pressure on the damage and permeability of coals were analyzed. Meanwhile,

the intrinsic mechanism of the influence of accelerated advance of working face on the damage and permeability of coals is revealed. The research has a certain theoretical significance for the prevention and control of coal and gas dynamic disasters and provides some references for the safety production in the field.

## 2 Experimental Procedures

### 2.1 Sample Preparation

There are many differences in mechanical properties between raw coal and coal briquette. In this work the raw coal samples were used in order to better represent the original characteristics of coals and conform to the actual field situation (Cao et al. 2010; Zhang et al. 2014). Raw coal samples were made from chunks of coal collected in Xinjing coal mine which is located in Yangquan mining area, Shanxi Province, China. The coal seam with an average thickness of 6.51 m is buried 540 m and the gas content is 8–11 m<sup>3</sup>/t. Chunks of coal were drilled, cut and polished to form cylindrical coal samples in accordance with ISRM standards (Fairhurst and Hudson 1999). The physical dimension of the coal samples is  $\phi 50 \times 100$  mm.

### 2.2 Experimental Apparatuses

In this work, the RLW-500G triaxial creep–seepage experimental system and PCI-2 AE test and analysis system are used to carry out the experiments. The experimental apparatuses are mainly composed of loading module, seepage module, temperature control module, and the safety protection module. The PCI-2 AE test and analysis system consists of sensors, amplifiers and multichannel acoustic emission system. Each experimental apparatus has been introduced in detail in previous papers, and will not be described in this paper (Wang et al. 2017b; Du et al. 2018). When mechanical tests are conducted under different stress paths, the permeability of the coal samples is measured synchronously, and the AE signal is monitored and collected in real-time.

### 2.3 Experimental Program

According to the change of the actual stress state of coal and rock during the advancement of the working

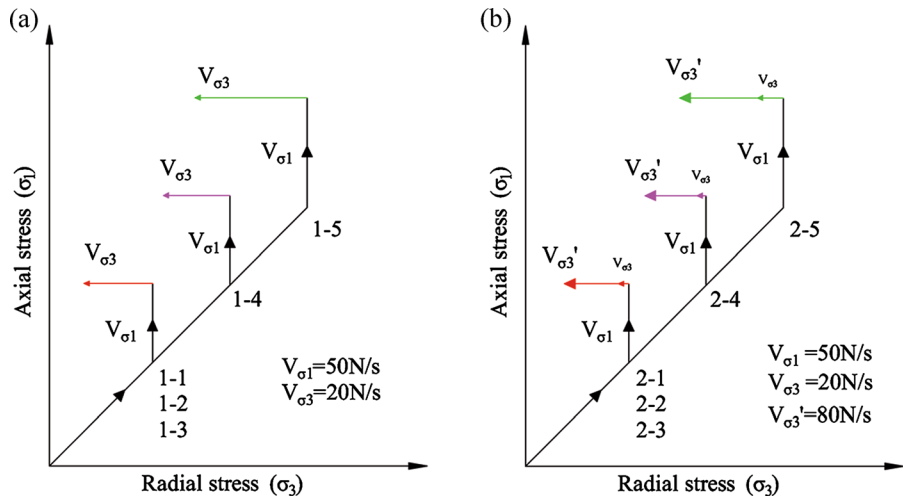
face, two mechanical paths, the conventional unloading confining pressure (UCP) and the accelerated unloading confining pressure (AUCP), are designed with some appropriate simplification. Due to the laboratory regulations, CO<sub>2</sub> is used instead of CH<sub>4</sub> in present work. Previous studies have shown that CO<sub>2</sub> and CH<sub>4</sub> have many similar properties and it will not affect the experimental analysis (Day et al. 2012; Busch and Gensterblum 2011; Gensterblum et al. 2013; Wang et al. 2017c). The two stress paths are shown in Fig. 1.

The detailed experimental schemes are as follows:

Path ① (UCP): Firstly, the axial stress and confining stress are simultaneously applied to 4, 7 and 10 MPa, respectively. After reaching the hydrostatic pressure state, the gas is injected into the samples. It is important to note that the gas pressures are different. When the hydrostatic pressure is 4 MPa, gas pressure is 1, 1.5, 2 MPa respectively. When the hydrostatic pressure is 7 and 10 MPa, the gas pressure is 2 MPa. Secondly, when the gas adsorption reaches equilibrium state, the confining stresses are kept invariant, and the axial stresses are applied to 62% of the peak strength of conventional triaxial compression at the rate of 50 N/s by force-controlled method. Meanwhile, the permeability and AE signal data are recorded simultaneously. The peak strength of conventional triaxial compression under the same condition is obtained through conventional triaxial compression tests. At last, the axial stress is kept fixed and the confining stress is unloaded at the rate of 20 N/s by force-controlled method. When the samples come to failure, the unloading rate is controlled by displacement-controlled method until the residual strength is stable. It is worth noting that the displacement-controlled method is only a method of controlling rate.

Path ② (AUCP): The first two stages are the same as those under UCP. Then, the axial stress is kept fixed and the confining stress is unloaded to 90% of the initial confining stress at the rate of 20 N/s by force-controlled method, then the rate is changed to 80 N/s. When the samples come to failure, the rate is controlled by displacement-controlled method until the residual strength is stable.

**Fig. 1** Stress paths: **a** UCP, **b** AUCP



### 3 Results

Based on the designed experimental scheme, the damage–permeability experiments of gas-bearing raw coal under accelerated unloading confining pressure condition were carried out, and the strength, damage, failure, seepage and time-dependent (Xu et al. 2018) characteristics of gas-bearing raw coal under different paths were analyzed.

#### 3.1 Strength Characteristics of the Gas-Bearing Coals

The stress–strain curves of gas-bearing coals under different initial conditions and different stress paths are shown in Fig. 2. It can be found that the compaction stage of stress–strain curve under each path is unobvious. The stress–strain curve mainly consists of elastic deformation, plastic deformation, yield failure and residual stress stage. Under different initial conditions and stress paths, the strength characteristics of the samples present significant differences. The main experimental results are shown in Table 1. In Table 1,  $\sigma_3$  and  $P$  represent the initial confining stress and gas pressure, respectively.  $\sigma_1$  is axial loading stress when the confining pressure begins to unload.  $V$  denotes the rate of unloading confining stress.  $\sigma_3'$  and  $\sigma$  represent the confining stress at failure and unloaded confining stress amount, respectively.  $N$  is the ratio of unloaded confining stress amount to the initial confining stress.

It can be concluded from Table 1 that with the same initial confining stress under UCP/AUCP paths, as the gas pressure increases, the confining stress at failure increases. Meanwhile, the unloaded confining stress and the ratio of unloaded confining stress to the initial confining stress decrease. Under the constant gas pressure, as the initial confining stress increases, the confining stress at failure increases, and the unloaded confining stress and the ratio of unloaded confining stress to the initial confining stress increase. Under the same initial conditions, compared with UCP path, the confining stress at failure increases under AUCP path, the unloaded confining stress and the ratio of unloaded confining stress to the initial confining stress decrease under AUCP path. Apparently, the sample is more susceptible to failure under AUCP path. Accelerated unloading confining stress makes the effective confining stress fall down more quickly and the mechanical and non-mechanical effects of gas (Viète and Ranjith 2007; Wang et al. 2017b, c; Masoudian et al. 2014) perform more rapidly. It is obvious that the samples respond faster to these effects. Under AUCP path, the stress state of sample is accelerated from triaxial stress state toward uniaxial stress state. The rapid reduction of effective confining stress causes the stored energy of the sample to be released in the radial direction, and the sample is accelerated to yield and failure under the combined actions of tension and shearing.

It can also be seen from Table 1 that with the same initial confining stress under AUCP path, as the gas pressure increases, the reduction magnitude of

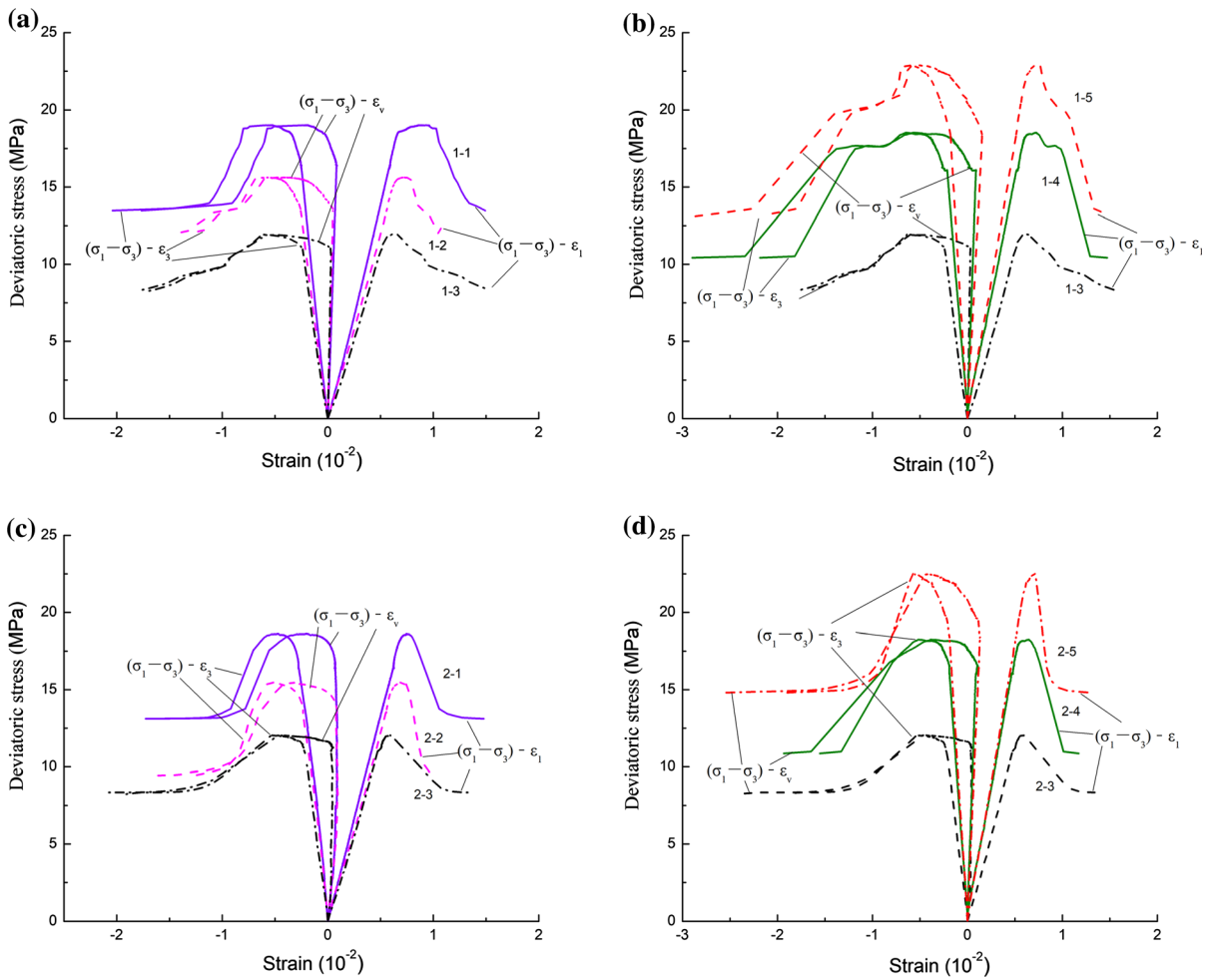


**Fig. 2** Stress–strain curves with different unloading paths: **a** UCP (with different gas pressure), **b** UCP (with different initial confining stress), **c** AUCP (with different gas pressure), **d** AUCP (with different initial confining stress)

**Table 1** Experimental results with different unloading paths

Paths	Sample number	$\sigma_3$ (MPa)	$P$ (MPa)	$\sigma_1$ (MPa)	$V$ ( $N\ s^{-1}$ )	$\sigma_3'$ (MPa)	$\sigma$ (MPa)	$N$ (%)
UCP	1-1	4	1	20.4	20	1.34	2.66	66.50
	1-2	4	1.5	17.5	20	1.85	2.15	53.75
	1-3	4	2	14.9	20	2.97	1.03	25.75
	1-4	7	2	23.1	20	4.42	2.58	36.86
	1-5	10	2	28.4	20	5.65	4.35	43.50
AUCP	2-1	4	1	20.4	20/80	1.51	2.49	62.25
	2-2	4	1.5	17.5	20/80	1.91	2.09	52.25
	2-3	4	2	14.9	20/80	3.02	0.98	24.50
	2-4	7	2	23.1	20/80	4.63	2.37	33.86
	2-5	10	2	28.4	20/80	5.99	4.01	40.10

confining pressure unloading ratio decreases from 4.25 to 1.25% when the sample is destroyed. Under the constant gas pressure, as the initial confining stress increases, the reduction magnitude of the ratio increases from 1.25 to 3.4%. It presents that under the constant initial confining stress, the effect of AUCP path on the samples is weakened as the gas pressure increases. On the other hand, under the same gas pressure, the greater the initial confining stress, the stronger the effect of AUCP path on the mechanical behavior of coal samples. Under these circumstances, the release of accumulated energy in the sample is more rapid and violent, and the sample is more susceptible to failure. Therefore, accelerated unloading confining stress has a significant controlling effect on the instability and failure of coal.

### 3.2 Results of Stress–AE–Seepage Experiments

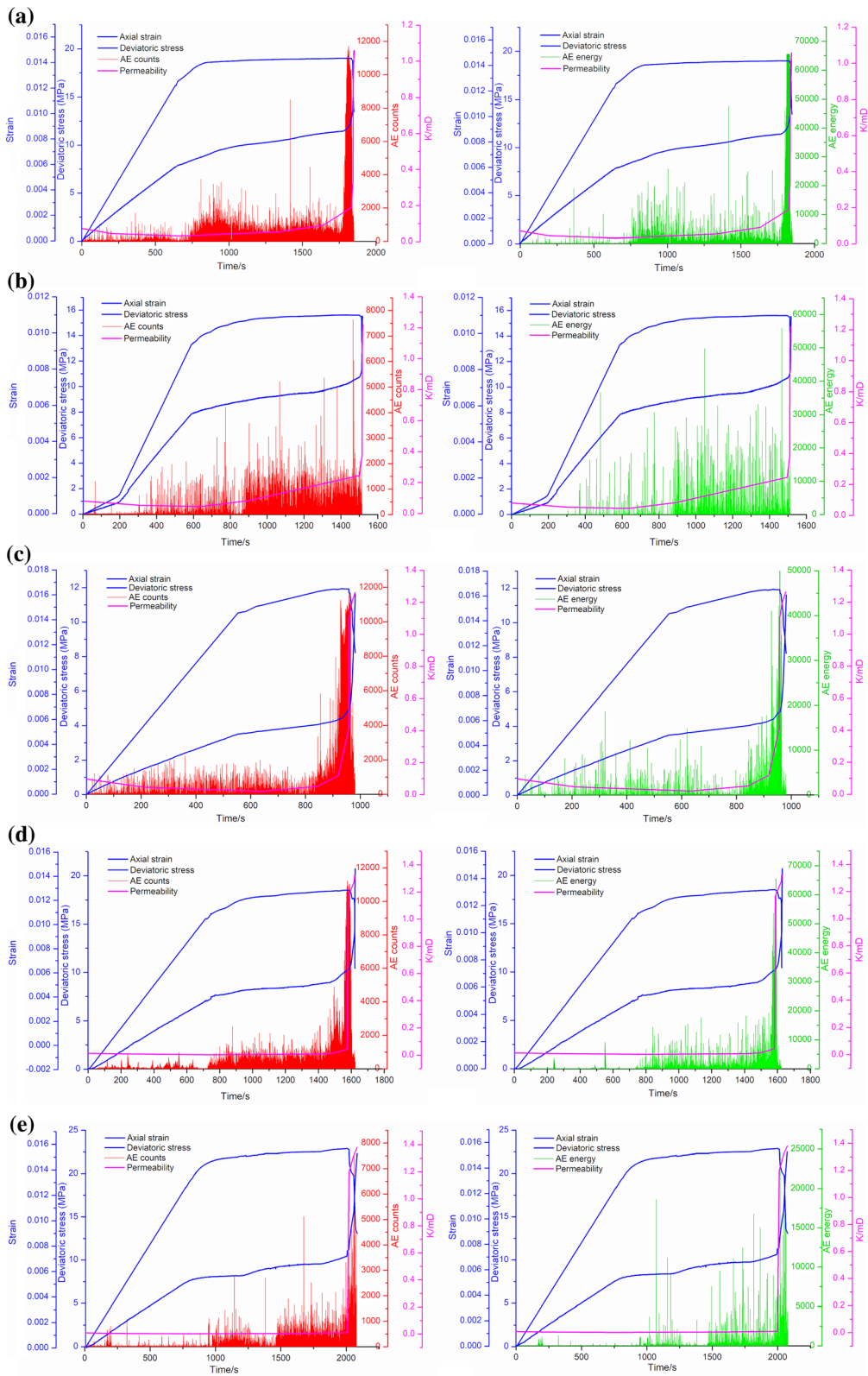
The experimental results of stress–AE–seepage under the two paths are shown in Figs. 3 and 4. There are several parameters used to characterize the damage degree of samples and the intensity of the AE events. In this study, AE count and AE energy are selected to reflect the damage evolution. It is important to note that the AE energy is a relative energy and it reflects the intensity of AE events. The unit of AE energy is  $\text{mV} \cdot \mu\text{s}$ .

As time goes by, the samples undergo a process from hydrostatic pressure state to failure state under the two paths, as shown in Figs. 3 and 4. Due to the different rates between axial loading and radial unloading, the deviatoric stress curve changes significantly. Meanwhile, under the action of the deviatoric stress, the axial strain gradually increases and the permeability undergoes four stages: rapid decrease, slow decrease, slow increase and sharp increase. The AE count and AE energy present four periods: slow change, rapid rise, sharp rise and stability. In the initial stage, the AE signal of the sample is low. When the sample is closing to the failure, the AE signal rises sharply, characterized by sharp damage as a whole. At the beginning of the whole process, as deviatoric stress increases, the coal sample is in the stages of compaction and elasticity. No significant damage appears in this stage. However, there are original pore and fracture structure in the coal, and the dislocation friction in the coal particles makes the AE count and AE energy change slowly. Then the coal sample is

plastically deformed, and the damage and crack in the coal are gradually developed. Therefore, the AE count and AE energy rise rapidly. When approaching and entering the stage of yield failure, the damage of the coal samples is further intensified until the entire failure with a through-crack forming, and the AE count and AE energy rise sharply. Afterwards, the AE signal gradually becomes stable. As pointed out by Xu et al. (2018), there is a lagging relationship between AE signal and stress–strain curve of the coal as a whole. However, it can be found from the figures that the axial strain, deviatoric stress and permeability have a good correspondence with AE signals. At the peak of the deviatoric stress, both the permeability and the AE signal increase sharply to the maximum.

It could be also found from the figures that the results of stress–AE–seepage experiments also have some significant differences between the two paths. Under the same conditions, compared with the UCP path, the time required for reaching failure under the AUCP path is significantly shorter, indicating that coal responds faster to the AUCP path and the coal sample is more susceptible to damage and failure under the AUCP path. The AE characteristics under the two paths are not exactly the same. Before the AE signal surges to the maximum, the AE count and AE energy under UCP are generally greater than that under AUCP under the constant conditions, and the surge magnitude of the AE signal under UCP is smaller than that under AUCP. It shows that under the same conditions, the sharp damage of coal under the AUCP path is more intense, and it is more violent when it is damaged. Under AUCP, the unloading of confining stress is accelerated, and there is not enough time for the crack developing in the coal. The sample is suddenly damaged when reaching its peak strength and the energy release is more violent and more powerful.

Under the AUCP path, provided that the initial confining stresses are the same, the time for failure is significantly shortened with the increase of gas pressure and the peak of AE count and AE energy are reduced. It further proves the mechanical and non-mechanical effects of gas on the coal. Under the fixed gas pressure, the time required for failure gradually increases with the increasing initial confining stress, and the peak of AE count and AE energy also have an increasing trend. When the initial confining stress is 10 MPa, the AE count and AE energy are low. It may be due to the



◀ **Fig. 3** Results of stress–AE–seepage experiments under UCP: **a** 4–1, **b** 4–1.5, **c** 4–2, **d** 7–2, **e** 10–2

differences in the original structure of the coal or the damage caused in sample preparation.

Under the AUCP path, the increase of permeability is significantly higher than that under the UCP path. This is mainly due to the fact that the release of energy is more violent and the impact is stronger, resulting in that the coal sample is damaged more severely under the AUCP path. Figure 5 shows the variation of coal permeability with different initial conditions under the AUCP path. Under the fixed initial confining stress, as the gas pressure increases, the axial strain decreases when the permeability surges. Moreover, the magnitude of the surge increases. Under the fixed gas pressure, as the initial confining stress increases, the axial strain increases when the permeability surges. Moreover, the magnitude of the surge also increases.

### 3.3 Failure Characteristics

The failure forms of gas-bearing raw coals under UCP and AUCP are shown in Figs. 6 and 7, respectively. Herein, 4–1 indicates that the initial confining stress is 4 MPa and the gas pressure is 1 MPa.

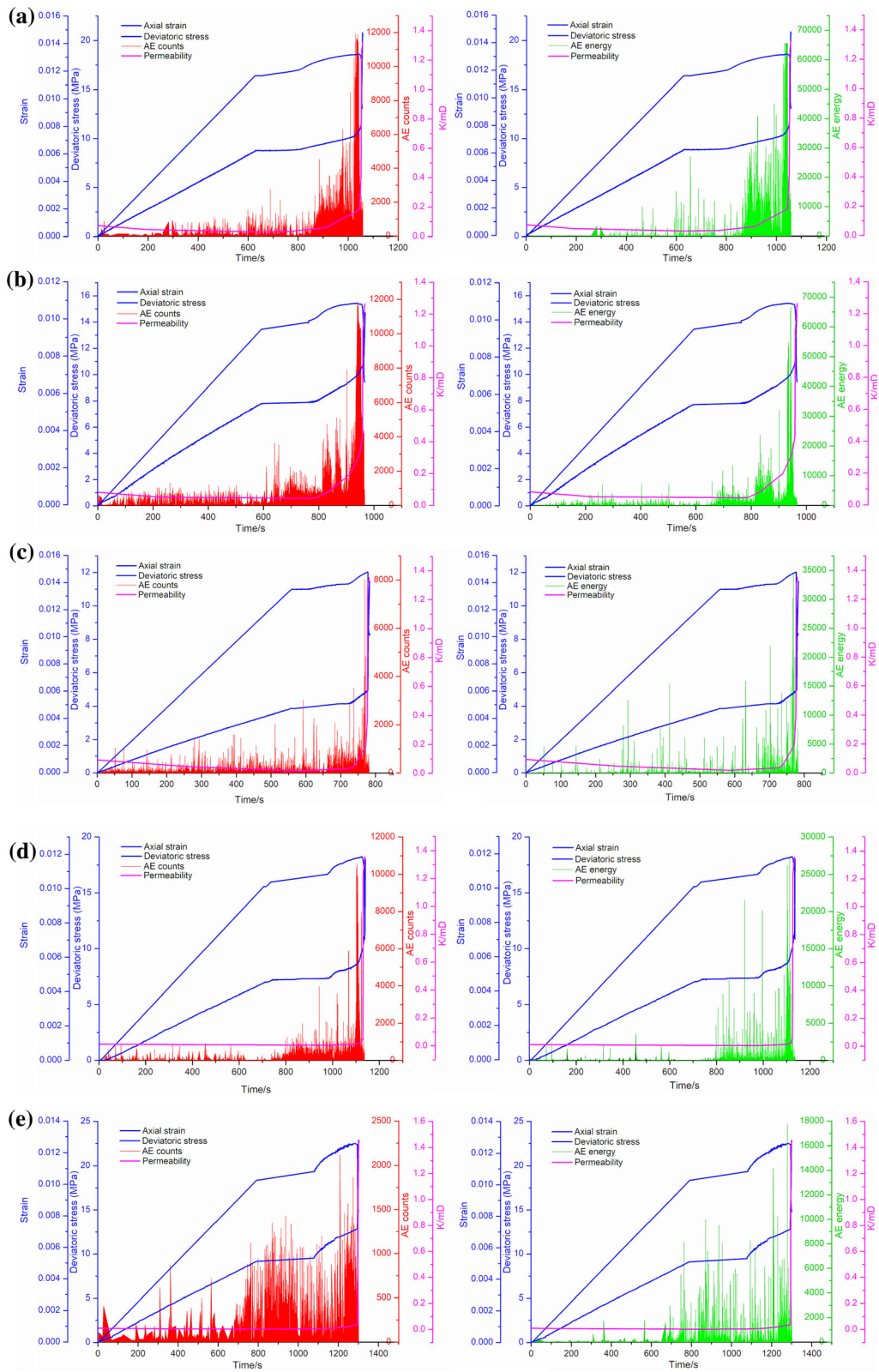
It can be concluded from above two figures that the failure forms of the raw coal samples under the different stress paths are similar. Under the two paths, due to the unloading effect, the stress state of the samples is gradually changed from the triaxial stress state to the uniaxial stress state. The reduction of the effective confining pressure causes the energy stored in the samples to be released in the radial direction. The compression–shearing effect is gradually transformed into tension–shearing effect, and the failure form of the sample is finally a tension–shearing failure. Under AUCP, the accelerated unloading of the confining stress rapidly reduces the effective confining stress. The release of radial energy is more severe. After failure, the samples presented more cracks and the degree of fragmentation is higher, which is consistent with the above analysis.

## 4 Discussion and Evaluation

Coal gas dynamic disasters have been threatening the safe and efficient production of coal mines. Their occurrence is related to the changes of ground stress, permeability and coal properties and so on. In the engineering construction, it is very important to improve work efficiency and cycle progress. However, the acceleration of the working face advancement is mainly manifested in the accelerated axial loading of the coal and rock or the accelerated radial unloading of the coal and rock in front of the working face, which has a significant impact on the mechanical response of coal and rock and the gas migration evolution. According to the law of stress redistribution in coal mining, during the process of advancing the working face, the stress-form of the roof rock presents periodicity. The acceleration of the advancing rate of the working face mainly leads to the accelerated unloading of the radial stress. In actual production activities, rockbursts and other dynamic phenomena often occur in underground engineering construction such as tunnel excavation. Coal and gas outburst accidents often occur in coal-uncovering through stone doors in mine roadway engineering. These projects are mainly based on the unloading of radial stress. The existed studies have shown that the unloading of radial stress has a greater impact on mechanical and seepage characteristics of coal than the loading of axial stress. Therefore, it is of great practical significance to study the damage and seepage characteristics of gas-bearing raw coal under accelerated unloading confining pressure. It could be seen in this work, under the accelerated unloading confining pressure path, the cracks in coal are not fully developed. Therefore, the elastic energy stored in coal is larger. Accordingly, the energy release during the failure is more intense and more violent, and the increase of permeability is also larger. After failure, the coal shows more broken characteristics. In the actual production, when the stress status of coal and rock are controlled by the combined effects of the accelerated loading of axial stress and the accelerated unloading of radial stress, the influence of the conclusion of this study will be further enhanced, and the risk of coal and rock dynamic disasters will be further increased.

The occurrence of coal and rock dynamic disasters is the result of a combination of various factors and the consequences are often extremely destructive. Under





◀ **Fig. 4** Results of stress–AE–seepage experiments under AUCP: **a** 4–1, **b** 4–1.5, **c** 4–2, **d** 7–2, **e** 10–2

of coal better developed, it is very necessary to control the reasonable rate of working face advancement.

the influence of mining disturbance, the stress concentration leads to the increasement of the elastic energy in the coal and further reduction of the permeability. When the stress in a certain direction is unloaded, the coal becomes unstable under the combined effects of the deviatoric stress and the gas pressure. Meanwhile, the energy is instantaneously released. The coal becomes broken due to the violent impact. In this work, we found that the acceleration of unloading rate makes this impact more intense and the release of energy more violent. Therefore, in order to avoid the concentration of stress and the aggravation of energy accumulation and to make the internal crack

### 5 Conclusions

1. Under two unloading paths, the sample presents the characteristics of rapid damage as a whole. The acoustic emission signals correspond well with the stress–strain and permeability changes of the coal samples. At the peak stress, the permeability and acoustic emission signal increase sharply to the maximum. The failure mode is tension–shearing failure. The unloading value of confining pressure and the unloading ratio when the coal is damaged decrease with the increase of gas pressure or with the decrease of confining pressure.

**Fig. 5** Variation of strain and permeability with different initial condition under AUCP: **a**  $\sigma_3 = 4$  MPa, **b**  $p = 2$  MPa

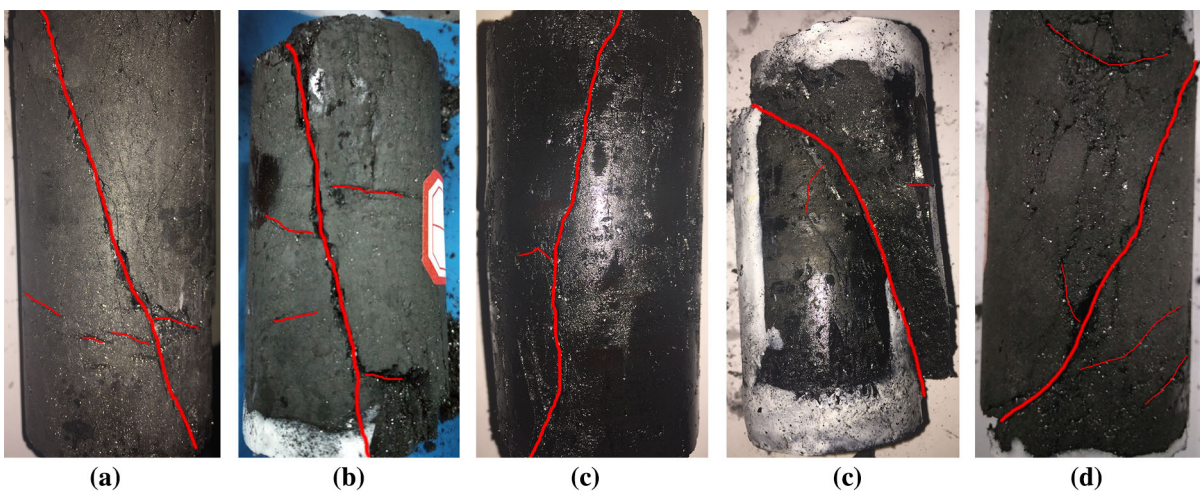
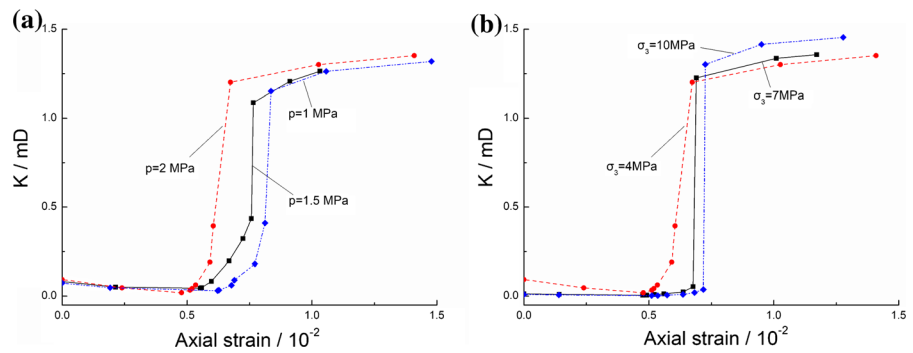


**Fig. 6** Failure forms of samples under UCP: **a** 4–1, **b** 4–1.5, **c** 4–2, **d** 7–2, **e** 10–2

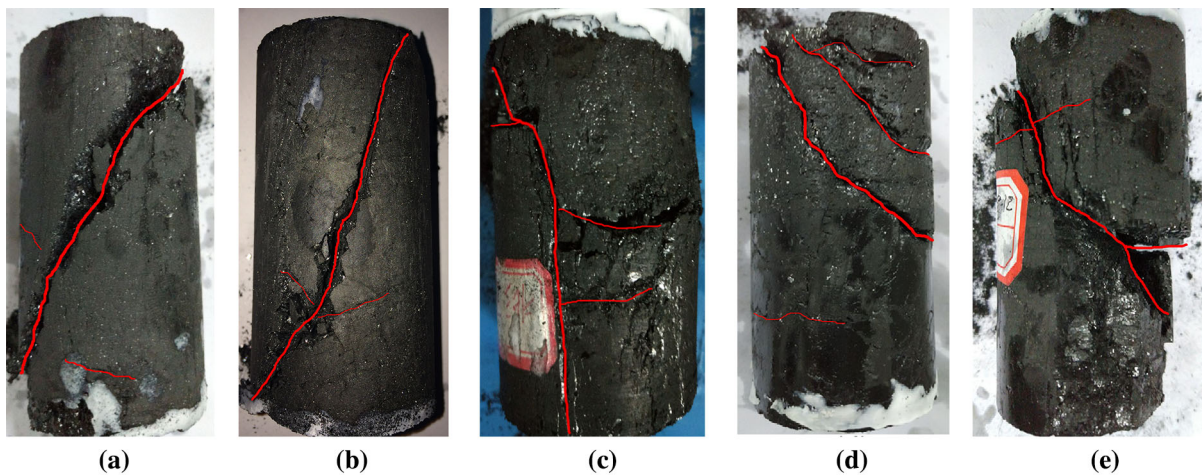


**Fig. 7** Failure forms of samples under AUCP: **a** 4–1, **b** 4–1.5, **c** 4–2, **d** 7–2, **e** 10–2

2. Compared with conventional triaxial unloading (UCP), the degree of rapid damage of coal body under AUCP is more significant. The time required for instability failure of coal body is obviously shortened and the permeability increment is obviously higher. When the sample is damaged, the unloading value and ratio of confining pressure is smaller in AUCP, and the sample shows more fragmentation and more impact destructive effect.
3. Under AUCP, with the increase of gas pressure, the axial strain decreases when the permeability increases sharply. Moreover, the increase magnitude of the permeability shows an upward trend. The time of coal damage is significantly shortened, and the influence of accelerated unloading mode on coal is weakened. With the increase of initial confining pressure, the axial strain increases when the permeability increases sharply. Moreover, the increase magnitude of the permeability shows an upward trend. The time required for instability and failure of coal body increases gradually, and the influence of accelerated unloading mode on coal is strengthened.

**Acknowledgements** This research is financially supported by the National Natural Science Foundation of China (51874314), the Open Funds of Hebei State Key Laboratory of Mine Disaster Prevention (KJZH2017K02), the Guizhou Science and Technology Support Program ([2017]2820), the Fund of China Scholarship Council (CSC), and the Yue Qi Distinguished Scholar Project, China University of Mining and Technology, Beijing. This study was funded by the State

Key Research Development Program of China (Grant Nos. 2016YFC0801402, 2016YFC0600708).

#### Compliance with Ethical Standards

**Conflict of interest** All the authors declare that they have no conflict of interest.

#### References

- Busch A, Gensterblum Y (2011) CBM and CO<sub>2</sub>-ECBM related sorption processes in coal: a review. *Int J Coal Geol* 87:49–71
- Cao S, Li Y, Guo P et al (2010) Comparative research on permeability characteristics in complete stress–strain process of briquettes and coal samples. *Chin J Rock Mech Eng* 29(5):899–906
- Chen HD, Cheng YP, Zhou HX, Li W (2013) Damage and permeability development in coal during unloading. *Rock Mech Rock Eng* 46:1377–1390
- Chen HD, Cheng YP, Ren T, Zhou HX, Liu QQ (2014) Permeability distribution characteristics of protected coal seams during unloading of the coal body. *Int J Rock Mech Min Sci* 71:105–116
- Day S, Fry R, Sakurovs R (2012) Swelling of coal in carbon dioxide, methane and their mixtures. *Int J Coal Geol* 93:40–48
- Du F, Wang K (2019) Unstable failure of gas-bearing coal–rock combination bodies: Insights from physical experiments and numerical simulations. *Process Saf Environ* 129:264–279
- Du F, Wang K, Wang G et al (2018) Investigation on acoustic emission characteristics during deformation and failure of gas-bearing coal–rock combined bodies. *J Loss Prevent Proc* 55:253–266
- Fairhurst CE, Hudson JA (1999) Draft ISRM suggested method for the complete stress–strain curve for intact rock in uniaxial compression. *Int J Rock Mech Min Sci* 36:281–289

- Fan C, Li S, Luo M, Du W, Yang Z (2017) Coal and gas outburst dynamic system. *Int J Min Sci Technol* 27(1):49–55
- Gensterblum Y, Merkel A, Busch A, Krooss BM (2013) High-pressure CH<sub>4</sub> and CO<sub>2</sub> sorption isotherms as a function of coal maturity and the influence of moisture. *Int J Coal Geol* 118:45–57
- Jiang C, Yu H, Duan M et al (2017) Experimental study of mechanical and permeability characteristics of coal with methane containing due to different loading–unloading speeds. *J Min Saf Eng* 34(06):1216–1222
- Lama RD, Bodziony J (1998) Management of outburst in underground coal mines. *Int J Coal Geol* 97:83–115
- Liu ZD, Cheng YP, Liu QQ, Jiang JY, Li W, Zhang KZ (2017) Numerical assessment of CMM drainage in the remote unloaded coal body: insights of geostress-relief gas migration and coal permeability. *J Nat Gas Sci Eng* 45:487–501
- Masoudian MS, Airey DW, El-Zein A (2014) Experimental investigations on the effect of CO<sub>2</sub> on mechanics of coal. *Int J Coal Geol* s128–s129(3):12–23
- Pan Z, Connell LD (2011) Modelling of anisotropic coal swelling and its impact on permeability behaviour for primary and enhanced coalbed methane recovery. *Int J Coal Geol* 85(3):257–267
- Qian MG, Xu JL, Wang JC (2018) Further on the sustainable mining of coal. *J China Coal Soc* 43(01):1–13
- Viete DR, Ranjith PG (2007) The mechanical behaviour of coal with respect to CO<sub>2</sub> sequestration in deep coal seams. *Fuel* 86:2667–2671
- Wang K, Du F (2019a) The classification and mechanisms of coal–gas compound dynamic disasters: a preliminary discussion. *Int J Min Miner Eng* 10(1):68–84
- Wang K, Du F (2019b) Experimental investigation on mechanical behavior and permeability evolution in coal–rock combined body under unloading conditions. *Arab J Geosci* 12(422):1–15
- Wang K, Du F, Wang G (2017a) Investigation of gas pressure and temperature effects on the permeability and steady-state time of Chinese anthracite coal: an experimental study. *J Nat Gas Sci Eng* 40:179–188
- Wang K, Du F, Zhang X et al (2017b) Mechanical properties and permeability evolution in gas-bearing coal–rock combination body under triaxial conditions. *Environ Earth Sci* 76(815):1–19
- Wang K, Du F, Wang G (2017c) The influence of methane and CO<sub>2</sub> adsorption on the functional groups of coals: Insights from a Fourier transform infrared investigation. *J Nat Gas Sci Eng* 45:358–367
- Wierzbicki M, Konečný P, Kožušníková A (2014) Permeability changes of coal cores and briquettes under tri-axial stress conditions. *Arch Min Sci* 59(4):1131–1140
- Wold MB, Connell LD, Choi SK (2008) The role of spatial variability in coal seam parameters on gas outburst behaviour during coal mining. *Int J Coal Geol* 75:1–14
- Xie H, Zhao X, Liu J et al (2012) Influence of different mining layouts on the mechanical properties of coal. *Int J Min Sci Technol* 22(6):749–755
- Xie H, Ju Y, Gao F, Gao M, Zhang R (2017) Groundbreaking theoretical and technical conceptualization of fluidized mining of deep underground solid mineral resources. *Tunn Undergr Space Technol* 67:68–70
- Xu C, Fu Q, Wang K et al (2018) Effects of the loading methods on the damage–permeability aging characteristics of deep mining coal. *J China Univ Min Technol* 1:197–205
- Xue Y, Ranjith PG, Gao F, Zhang D, Cheng H, Chong Z, Hou P, Xue Y, Ranjith PG, Gao F (2017) Mechanical behaviour and permeability evolution of gas-containing coal from unloading confining pressure tests. *J Nat Gas Sci Eng* 40:336–346
- Yin G, Jiang C, Wang JG, Xu J (2015) Geomechanical and flow properties of coal from loading axial stress and unloading confining pressure tests. *Int J Rock Mech Min Sci* 76:155–161
- Zhang ZG, Cao SG, Guo P et al (2014) Comparison of the deformation characteristics of coal in gas adsorption–desorption process for raw and briquette coals. *J China Univ Min Technol* 43(3):387–394
- Zhang Q, Fan X, Liang Y, Li M, Li G, Ma T, Nie W (2017) Mechanical behavior and permeability evolution of reconstituted coal samples under various unloading confining pressures—implications for wellbore stability analysis. *Energies* 10(3):292
- Zhang MB, Lin MQ, Zhu HQ, Zhou DH, Wang LK (2018a) An experimental study of the damage characteristics of gas-containing coal under the conditions of different loading and unloading rates. *J Loss Prev Proc* 55:338–346
- Zhang D, Yang Y, Wang H et al (2018b) Experimental study on permeability characteristics of gas-containing raw coal under different stress conditions. *R Soc Open Sci* 5(7):180558

**Publisher's Note** Springer Nature remains neutral with regard to jurisdictional claims in published maps and institutional affiliations.